metals

MDPI

Article

MECHANICAL PROPERTIES OF CoCr DENTAL-PROSTHESIS RESTORATIONS MADE BY THREE MANUFACTURING PROCESSES. INFLUENCE OF THE MICROSTRUCTURE AND TOPOGRAPHY.

R. Padrós [1], M. Punset [2,3,4], M. Molmeneu [2,,4], A. Brizuela [5] and M. Herrero-Climent[6], E. Rupérez[2], FJ. Gil [7,8*]

[1] Barcelona Dental Institute. Barcelona, Spain.
[2] Biomaterials, Biomechanics and Tissue Engineering group (BBT), Department of Materials Science and Engineering. Universitat Politècnica de Catalunya (UPC). Av. Eduard Maristany 16, 08019-Barcelona. Spain.
[3] UPC Innovation and Technology Center (CIT-UPC), Technical University of Catalonia (UPC), C. Jordi Girona 3-1, 08034 Barcelona, Spain.
[4] Barcelona Research Centre in Multiscale Science and Engineering, Technical University of Catalonia (UPC), Av. Eduard Maristany, 10-14, 08019 Barcelona, Spain
[5] Department of Surgery and Medical-surgical Specialties, University of Oviedo. Oviedo. Spain.
[6] Porto Dental Institute, Porto, 4150-518, Portugal;
[7] Bioengineering Institute of Technology, International University of Catalonia, Josep Trueta s/n. 08195-Barcelona, Spain.
[8] School of Dentistry, Faculty of Medicine and Health Science, Universitat Internacional de Catalunya (UIC), C. Josep Trueta s/n, 08195 Sant Cugat del Vallès, Spain
* Correspondence: xavier.gil@uic.cat.

ABSTRACT: The aim of this study is to compare the mechanical properties of three different dental restorations´ manufacturing processes (CADCAM milling, casting and laser sintering) generated by only one laboratory scanner focusing on marginal fit analysis and their mechanical properties. Chrome-cobalt (Cr-Co) alloy from the same batch was used for three different methods to made an implant abutment simulating a maxillary right first molar was fixed in hemi-maxillary stone model Five scans were performed by each tested and 9 frameworks were manufactured for each manufacture procedure. Field emission Scanning electron microscope (FE-SEM) direct vision was used to marginal gap measurement in five critical-points for each specimen. In order to fix the samples in the microscope chamber, the restorations were submitted at a compression load of 50N. The samples always have the same orientation and conditions. The resolution of the microscope is 4 nm and it is equipped by J image software. Microstructure of the samples was also determined with the FE-SEM equipped with EDS-microanalysis. Roughness parameters were measured using White Light Interferometry (WLI). The arithmetical mean for R_a and R_q of each sample was calculated. The samples were mechanically characterized by means of microhardness and flexural testing. Servo-hydraulic testing machine was used with cross-head rate of 1mm/min. Two-way ANOVA statistical analysis was performed to determine whether the marginal discrepancies and mechanical properties were significantly different between each group (significance level $p < 0.05$). The overall mean marginal gap values were: from 50.53 ± 10.30 μm for the samples produced by CADCAM to 85.76 ± 22.56 μm for the samples produced by the casting method. Laser sintering presents a marginal gap of 60.95 ± 20.66 μm. The results revealed a statistically significant difference (p-value < 0.005) in the mean marginal gap between the CADCAM systems studied. The higher flexure load to fracture for these restorations were for CADCAM restoration and lower was for the casting samples. (For these restorations CADCAM Restoration yielded higher flexure load to

fracture and Casting ones yielded lower). Porosity and the microstructure play a very important role on the mechanical properties.

Keywords: CAD-CAM milling; casting; laser sintering; Additive Manufacturing; marginal fit; Cr-Co alloy; dental prosthesis; dental restorations; mechanical properties; roughness; flexural load to fracture; hardness

1. INTRODUCTION

Over the last decade, the dental restorative sector has probably undergone the biggest technological revolution throughout its history. The continuous appearance of new technologies in both, digital and manufacturing industries, has enabled continuous improvement throughout R+D+I in order to overcome the drawbacks of conventional manufacturing processes.

The aforementioned revolution of manufacturing processes has been accompanied by a parallel digital technology revolution, along with also near-immediate implementation of new-developed procedures based on digital technologies [1-5]. As a result, digital dentistry revolution involved rapid implementation of newly-developed technologies such as 3D-Imaging [3, 6], computer-aided design (CAD) [1,4,7-8], computer-aided manufacturing (CAM) [9-10], intraoral scanning [3,6], cone-beam computer tomography (CBCT) [11-15], x-ray computer micro tomography (μ-CT) [16-17], and computer-aided implantology [2, 18], among the most relevant.

In summary, manufacturing processes have evolved over time from traditional methods, with a high-level handicraft production component based on classic conformation methods (casting, plastic deformation and subtractive methods), to automated computer-aided methods with a high degree of technical sophistication using leading-edge technologies. For this latter group of state-of-the-art processes, two main families of computer-aided processes must be highlighted, computer-aided design and milling subtractive systems (CADCAM) and computer-aided design and fabrication additive manufacturing methods (AM).

Digital dentistry is continually growing from the casting process. From wax lost method for manufacturing frameworks for dental restorations, to the use of CADCAM technology. The evolution to digital processes avoids many mistakes and the dependence of the laboratory technician's ability [18-20]. The use of digital processes achieves better accuracy following the workflows stages: scanning, design and manufacturing. In recent years, new procedures and technologies, along with advanced new materials have helped the introduction of new methodologies to produce dental restorations [1-5].

The combination of advanced technology in both, digital techniques and automated computer-integrated manufacturing systems, has led to a great leap forward in both oral implantology and dental restoration sectors also known in the field of dentistry as Digital Dentistry or Dentistry 3.0 [10]. As a result, there is a wide range of technologies currently available for CoCr dental restoration manufacturing. Some of them based on subtractive manufacturing methods such as CADCAM milling (CADCAM) systems [7-10], and the rest ever-expanding remaining group of processes based on additive manufacturing methods such as direct metal laser-sintering systems (DMLS) occasionally referred to as selective laser sintering (SLS) or selective laser melting (SLM) [21-23], Metal Injection Molding (MIM) [24], Electron Beam Melting (EOS) [25] and Laser Engineering Net Shaping (LENS) [26], among the highlights.

The newly state-of-art implemented technologies would theoretically enable overcoming the intrinsic limitations of conventional manufacturing techniques (machining, casting, forge and pressing). Some of the more important limitations would include high tolerance, low adjustment and dimensional accuracy, limited capacity to the production of complex shapes, low volumes of production, consequently leading to high associated product manufacturing costs

For the long-term framework behavior perspective, it is very important to take into account some key-factors such as the quality of surface finishing, marginal accuracy, mechanical properties,

corrosion resistance, ion-release behavior, and of course biocompatibility [27–31]. One of the most important aspects is the accuracy, the minimization of the gaps and high precision in the adjustment of the structures [32-41]. Discrepancies in the marginal fit can produce recurrent caries, plaque accumulation, periodontal diseases or fracture of the dental restoration [42-48].

Many researchers have been focusing their efforts on evaluating the gap size effect on dental restoration functional behavior in order to determine and finally set a gap critical-size acceptance limit value for clinical use. However, gap value strongly depends on both measuring and manufacturing methods used. Currently there is no general consensus regarding an acceptable tolerance limit. As a result, general consensus has not been found in the bibliographical surveys realized, which has revealed a high level of discrepancy in the range of 35 to 120 μm [44-45, 49]. In the same way, with regards to accuracy, there is neither a specific limit value nor a general consensus amongst researchers in this area. Some works reported the best results were yielded by the CADCAM systems, others by laser sintering or even through traditional casting techniques, other authors didn't find substantial differences between these systems [50-51]. The marginal fit has a key role in the dental restoration success and the new strategic objective (goal) would be focused on achieving a maximum gap value in the range of 25 to 50 μm to ensure good behavior [52-55].

Different methodologies have been used to evaluate the marginal gaps and the fitting of prosthetic dental restorations over time, including optical microscopy [56], profile projector [10], micro-CT [13-15] or laser videography [30], with different results. For this research the measurements have been realized by High Resolution Field Emission Scanning Electron Microscope (HR-FSEM) with more than 100 measures for each model. Samples were fixed and observed with the same position and orientation in all cases. The same batch of the CoCr alloy avoids the influence of different materials tested on the results. Furthermore, flexure load to fracture of CoCr frameworks has been also determined for all manufacturing methods evaluated, and the influence of the marginal fit and the microstructure were also studied/evaluated. Furthermore, the originality of this contribution is also the determination of the influence of the microstructure of the material obtained by each manufacturing process on the mechanical properties, surface quality and the defects of the prosthesis.

2. MATERIALS AND METHODS

2.1. Model preparation

A master model was obtained from a real clinical situation: the replacement of an absent (pontic) tooth (FDI nº15) with the construction of a fixed partial denture on natural abutments (FDI nº14 and 16) with three elements.

The natural teeth were prepared with a 1,2mm deep 90º finish line around the contour of the abutments (360º), with a convergence angle of the walls of approximately 10º. The termination line, being natural teeth, was more apical in the vestibular and palatar areas.

An impression of abutment teeth was made using an addition silicone 3M Express tm 2 Penta with double viscosity (3M, Minnesota, USA). The impression was poured to obtain a master cast using Diemet-E epoxy resin (Erkodent™ Erich Kopp, Pfalzgrafenweiler, Germany). Subsequently, the master cast was duplicated, obtaining 18 working models.

Duplication procedures were performed in a room with humidity and temperature conditions within the following limits: 70-80% and 23-25ºC respectively. All the models were made in Diemet-E epoxy resin by the same operator and following the same working sequence protocol from a silicon index key Wirosil™ Duplicating Silicone (BEGO Herbst GmbH & Co, Bremen, Germany) and respecting the manufacturer´s instructions. The procedure was repeated until 18 models free of pores and imperfections were obtained.

2.2. Study Groups assignment

The models were divided in three groups:

- Group A: Cr-Co frameworks manufactured using wax-lost casting method. A total of 9 models were performed (n=9).

- Group B: Cr-Co frameworks manufactured using a 5-axis CADCAM milling system. A total of 9 models were performed (n=9).
- Group C: Cr-Co frameworks manufactured using Laser Sintering system. A total of 9 models were performed (n=9).

2.3. Structure design and CAD-CAM manufacturing

Models were digitalized using a desktop optical scanner Imetric (Imetric 3D SA, Geneva, Switzerland)) in a dental laboratory (Archimedes Pro™, La Seu d'Urgell, Spain). Structures were computer-designed using specific software for prosthodontic design Exocad™ (Exocad GmbH, Darmstadt, Germany) respecting the following specifications:

- Thickness of 0,5mm around the entire outline of the structure.
- Pontic in FDP position (nº15) with a convex shape on its cervical surface and 1 mm away from the edentulous crest.
- Application of a space of 50 μm on the dies to 1mm form the location of the finishing line.

Nine samples (n=9) were manufactured by CADCAM system using 5-axis Zfx-Sauer-10 milling cutter unit machine (Zimmer, Dachau, Germany), nine samples (n=10) were manufactured by means of casting using lost-wax technique with coating of phosphate and nine were manufactured by laser sintering method using a DLMS machine EOSINT M270 (EOS, Munich, Germany). The feedstock CoCr powder material used was powder with particle size in the range from 0.01 to 0.1 mm in diameter. Samples were verified in terms of both dimensions and volume of the structure.

These frameworks were not cemented. All structures were made of Cr-Co alloy (Dentaurum Gmbh&Co, Ispringer, Germany) (Figure 1) with the same chemical composition in all cases, which was determined by energy dispersive x-ray spectroscopy (EDS) microanalysis. Co Cr alloys are the most used in the dental restorations. One of the most interesting properties of this alloy is its wide melting temperature range that avoids distortion of the structures. The chemical composition in weight percentage is shown in Table 1.

Table 1. Chemical composition of CoCr alloy (%wt).

Chemical Element	Co	Cr	W	Si	C	Nb
(%wt)	56,53 ± 2.11	27,11± 1.31	9,64± 0.79	1,27 ± 0.80	< 1%	< 1.5%

The size of the Co-Cr powder (Remanium Star CL, Dentaurum, Ispringen, Germany) was 10–40 μm in diameter with a coefficient of thermal expansion is 14.1 10-6 K-1 and with a melting temperature around 1495ºC [57].

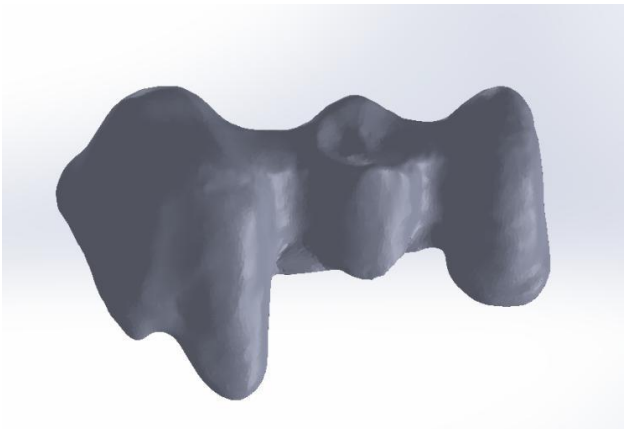

Figure 1. 3D-CAD model of CoCr dental restoration evaluated.

2.4. Surface Roughness

Roughness measurements were made using non-contact White-light (WLI) optical interferometry (Wyko NT1100 Optical Interferometer, Veeco Instruments, Plainview, NY, USA), in vertical scanning interferometry mode at x10 to x100 magnification. The interferometric technique is ideal for imaging these surfaces as a large area of the surface can be imaged with a high vertical resolution (≈2 nm). The analysis area was 63 x 47 μm. Data filtering and analysis were performed with specific image analysis software (Wyko Vision 32; Veeco Instruments). A Gaussian filter was used to eliminate tilt from every surface analysis in order to separate waviness and form from roughness. The amplitude parameter (Sa) and the Index area (SA Index) were evaluated for three different specimens of each group of samples. Two samples of each type and 4 zones in each sample were analyzed. Ten roughness measures were obtained for each sample.

2.5. Surface morphology and marginal gap determination.

Surface morphology and composition were analyzed by means of high-resolution Field Emission Scanning Electron Microscopy (HR-FSEM) using a Neon 40 Surface Scanning Electron Focused Ion Beam Zeiss (Zeiss, Germany) equipment with GEMINIS and Image-J software was used for dimensional measurement analysis.

In order to fix the sample in the microcopy chamber, the models were anchored with clamps and a 50N load was applied to the middle of the model in order to ensure proper fixation. Load was always applied in the same position and direction to have exactly the same angle between the model and the electron beam. This load is applied in order to avoid micromovements which could affect to the measurements. This load (50 N) does not produce plastic deformation or damages in the model. This method is according to the Holmes et al. and Affy et al. [58-59]. A scheme can be observed in Figure 2.

Gap discrepancies were determined in three areas of the vestibular regions as well as in two areas of the palatal regions, as can be observe in Figure 2. The points are random and these are taken every 1 micrometer to the right and to the left up to a distance of 500 micrometers from the point to the right and 500 micrometers to the left. Therefore, for each point 1000 measurements are taken. These distances and the operation distances are controlled by the software of the microscope.

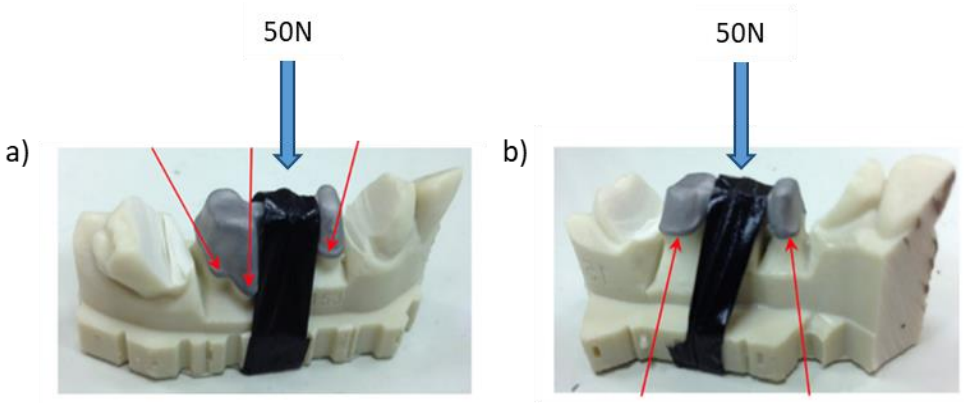

Figure 2. Images showing both interior and exterior regions of interest for accuracy measurement, as well as defining the point of load application and he direction of the applied load: a) Outer region with three regions of interest and b) Inner region with two regions of interest.

2.6. Mechanical Testing

Hardness distribution in a cross-section of specimens was measured using a Akashi Vickers microhardness tester model MVK-H0 (Akashi, Matsusawa, Japan) with a load of 1 Kgf for a dwell loading time of 15 s.

To measure the flexural loag to fracture on dental structures there is no international standard. For this reason and according to the methods of other authors simulating the real case [60-62], 3-point bending tests were performed.

Mechanical testing grips have been precision engineered in order to be able to carry out the load application on the manufactured samples as close as possible to the real conditions [63]. In addition, mechanical grips have also precision designed and manufactured in order to ensure a perfect accommodation of samples during 3-point flexure tests. With regard to the starting material used for the manufacture of testing grips, highly resistant refractory steel has been selected in order to avoid any deformation during mechanical tests. Samples were grip-fixed in a cantilever configuration. Load application was axially conducted by pointed tool attached to upper grip, which was perpendicular aligned to the horizontal-axis of the framework, with a single point of contact located in the middle of the restoration (Figure 3b). The length of the clamp was 26 mm and the point where the load is applied was in the middle (13 mm) from the ends. Mechanical assays were performed using a universal servo-hydraulic testing machine, Bionix model 370 (MTS, USA) (Figure 3c) equipped with a load cell of 25 KN. The equipment was controlled by means of a PC-interface by using software TESTAR II ® (MTS, USA). Mechanical tests were conducted using a constant cross-head rate of 1mm/min for all tests.

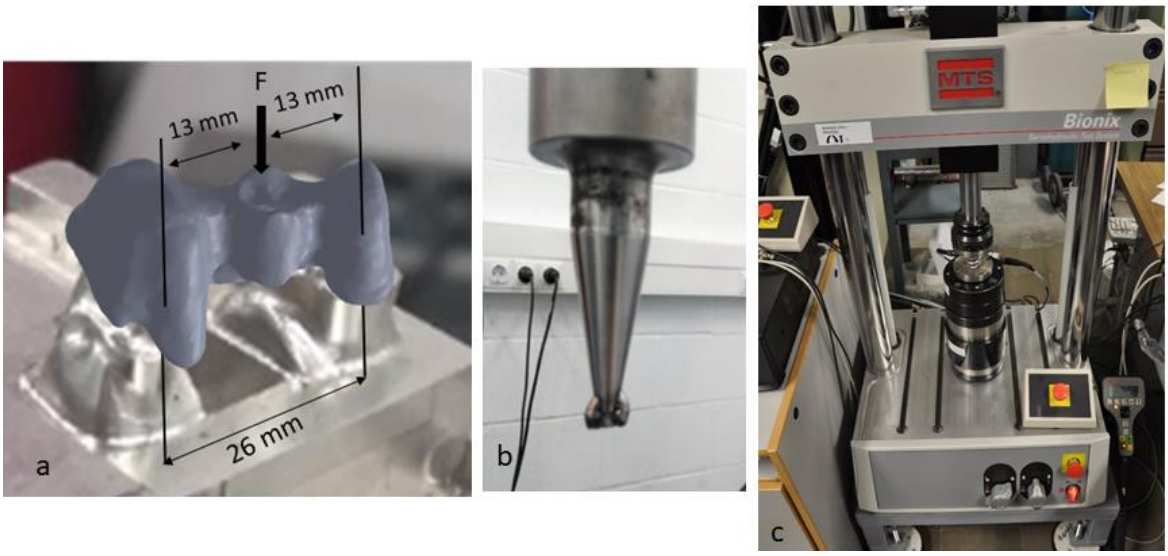

Figure 3. Overall 3-Point Flexure test set-up. a) Lower clamp used for sample positioning, b). Upper clamp used for load application, c) MTS Bionix 370 Servo-hydraulic universal testing machine.

2.7. Statistical analysis.

Means and standard deviations of both Sa and SA Index surface topography parameters, as well as gap, were determined for all group of samples. T-Student and one-way ANOVA tests (α=.05) were used to assess the influence of the manufacturing process on both the roughness parameters and gap. The differences were considered to be significant when $p < 0.05$.

All statistical analyses were done with a statistical software package (Minitab; Minitab Inc) by using MinitabTM software (Minitab release 13.0).

3. RESULTS

The SEM analysis of marginal gap performed in 135000 measurements —i.e., 5000 measurements for each sample analyzed at a rate of 1000 measurements for each of the 5 areas of interest evaluated. Figure 4 shows examples of the different accuracy for three samples obtained by CADCAM, casting and laser sintering. mean values for the CADCAM system studied. Figure 5 shows the different mean gap values (marginal fit) obtained by all manufacturing methods, which values are summarized in Table 2. The results present statistical significance differences between the three different processes ($p<0.05$).

The mean values and the standard deviations of all properties evaluated (the Vickers hardness, marginal Gap, Surface roughness and area index, as well as flexure load and deflection to fracture) are summarized in Table 2.

Table 2. Marginal gap, roughness, hardness and mechanical properties test results.

Properties / (units)	Manufacturing Process / Results (mean ± STD)		
	CADCAM	Casting	Laser Sintering
Marginal Gap, (µm)	50.53 ± 10.30	85.76 ± 22.56	60,95 ± 20.66
Sa (nm)	731.27± 19,0	796.60 ± 19,8	859.5 ± 18,9
SA Index area	2,1± 0,1	2,2 ± 0,1	1,8 ± 0,1
Hardness, (HV)	356 ± 20	390 ± 15	473 ± 25
Flexural load to fracture, (N)	6813± 169	6291 ± 105	5422 ± 302
Deflection to fracture, (mm)	4,10 ± 1,12	2,55 ± 1,21	3,75 ± 1,10

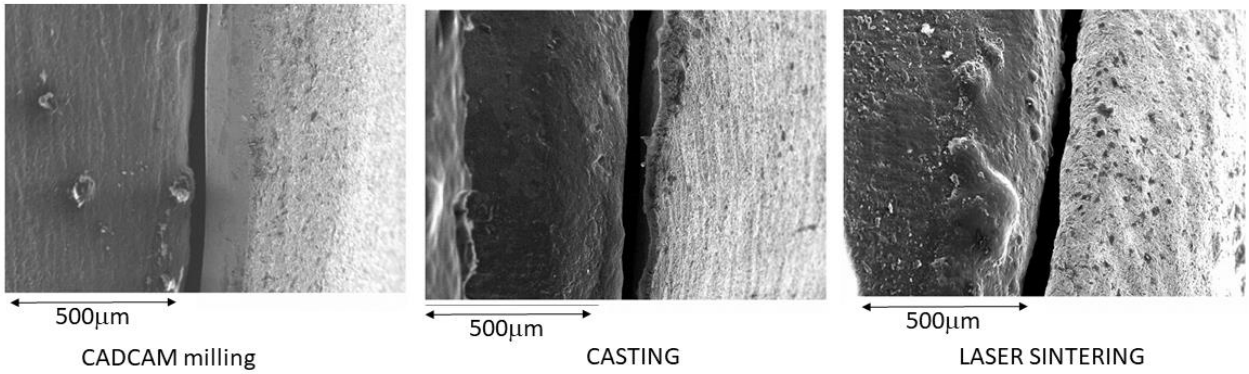

Figure 4. SEM-Micrographs of GAP measurement obtained by different processes.

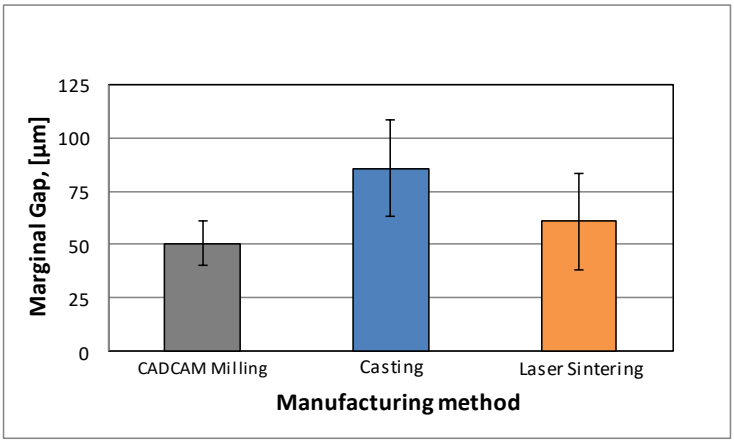

Figure 5. Marginal accuracy for the dental restoration manufactured by different methods.

Roughness measurements results confirmed the better surface finishing of CADCAM milled as compared with the rest of the evaluated processes, casting and laser sintering, as seen in Figure 6. As shown on Figure 6, the results of roughness measurements confirmed CADCAM Milled had better surface finishings in comparison to the other evaluated processes (casting and laser sintering) Figure 7 shows the 3D topography maps of samples manufactured by all studied methods. These results have statistical significant differences between each manufacturing system.

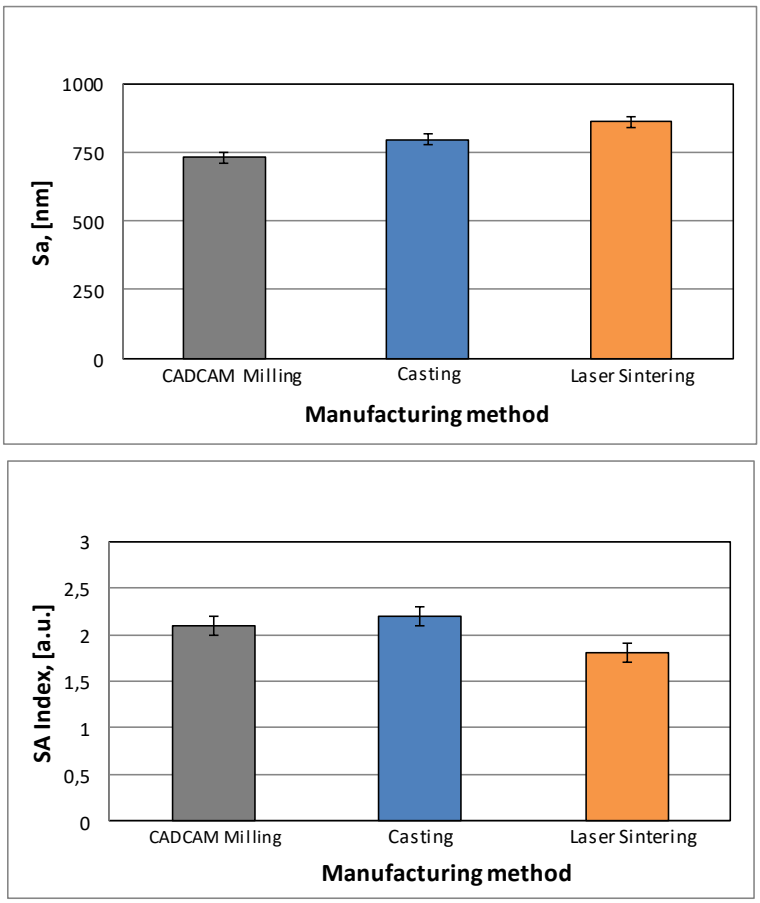

Figure 6. Results of roughness (Sa) and the surface area index for the different dental restorations.

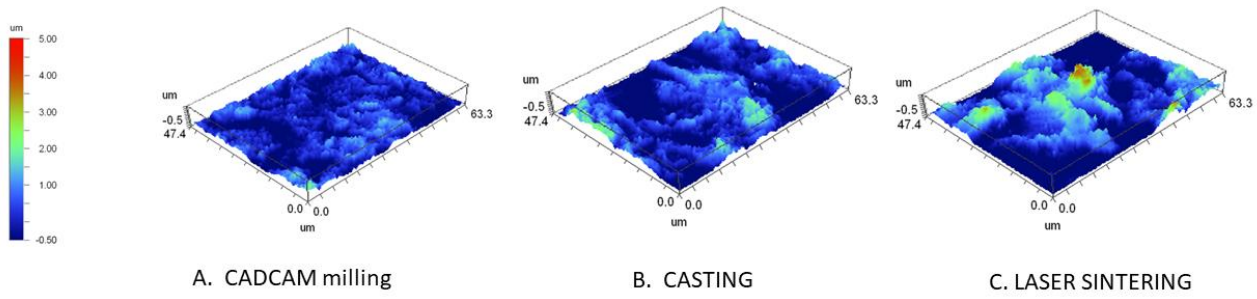

Figure 7. 3D topographic maps of three different models obtained by WLI method: a) CADCAM milling, b) Casting, and c) Laser sintering.

The results of microhardness are shown in Figure 8. The results present statistical significance differences between them.

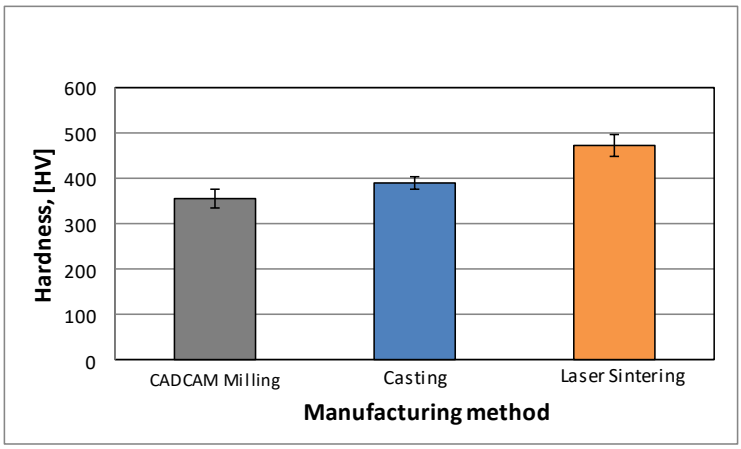

Figure 8. Microhardness (HVN) for the samples obtained with different methods.

Both, flexural load to fracture and deflection to fracture results obtained for each fabrication method are shown in Figure 9. Flexural load to fracture presented statistically significant differences between them. The small standard deviations are indicative of the high degree of reproducibility achieved by all manufacturing methods. However, the same comparison in terms of deflection to fracture did not present statistically significant differences.

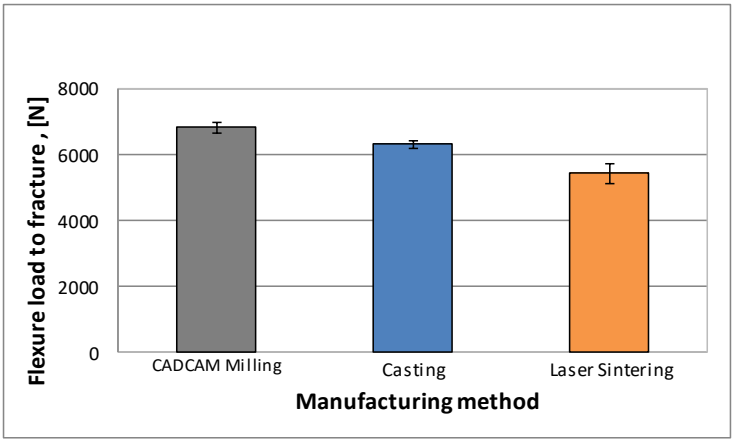

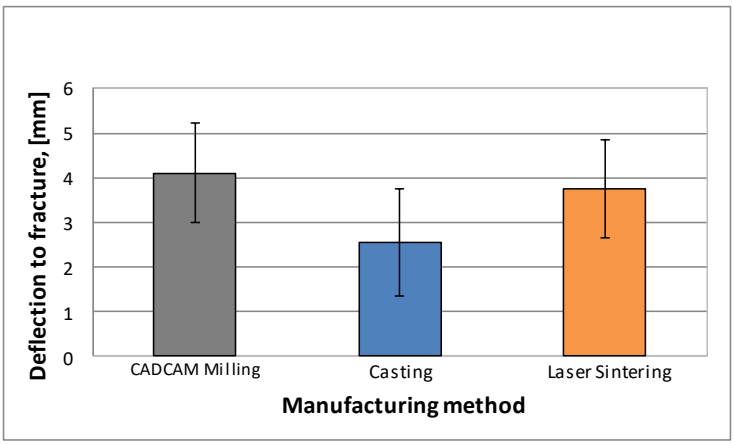

Figure 9. Flexural load to fracture and deflection to fracture obtained by three point bending for each dental restoration method.

The microstructural analysis of manufactured samples would explain the differences in the mechanical properties obtained. Figure 10a shows a sample obtained by CADCAM milling, we can observe the machining marks on the surface without porosity.

As seen in figure 10b, CADCAM milled samples presented a highly homogeneous microstructure characterized by the presence of uniform equi-axial grains with large quantities of twins inside. This equiaxial microstructure revealed that the material has been subjected to prior annealing heat treatment, which was realized in order to remove the internal stress generated during the material's production. Additionally, the presence of twins inside the crystalline grains might be related to the residual stresses generated during the CADCAM milling process. The as-received material has been submitted to cold worked and consequently the material does not present porosity, voids or cracks which could decrease the mechanical properties. In view of the results, the microstructure of CADCAM milled samples mainly depended on the initial microstructure of the as-received pre-manufactured block.

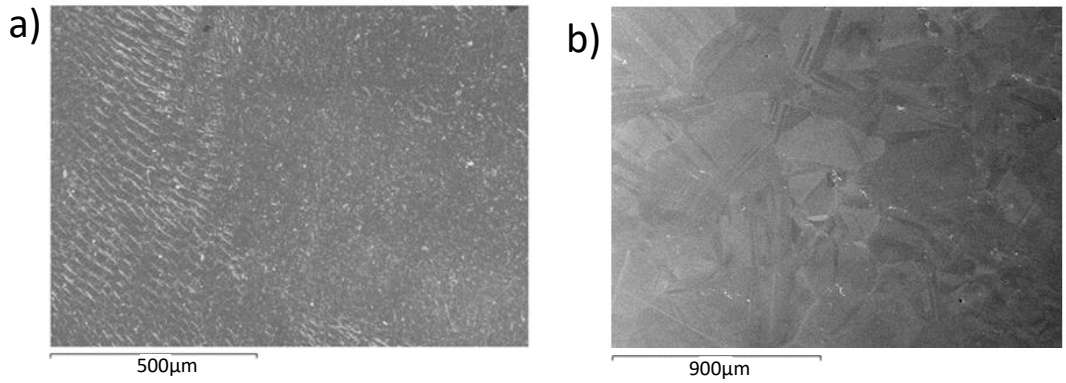

Figure 10. Microstructure and surface defects of CADCAM milled samples: a) machining marks and b) equiaxial grains with twins inside.

In Figure 11a, the surface of a sample obtained by laser sintering can be observed. The welding seams produced along the sintering path described by the laser beam is clearly identified. Besides, the surface analysis also revealed the presence of several porous with many particles inside, as seen in Figure 11b. Furthermore, an in-depth analysis of this porosity has shown a clear alignment between pores. These defects have a negative influence on the mechanical properties of laser sintered components, which can lead to significant anisotropic mechanical behavior.

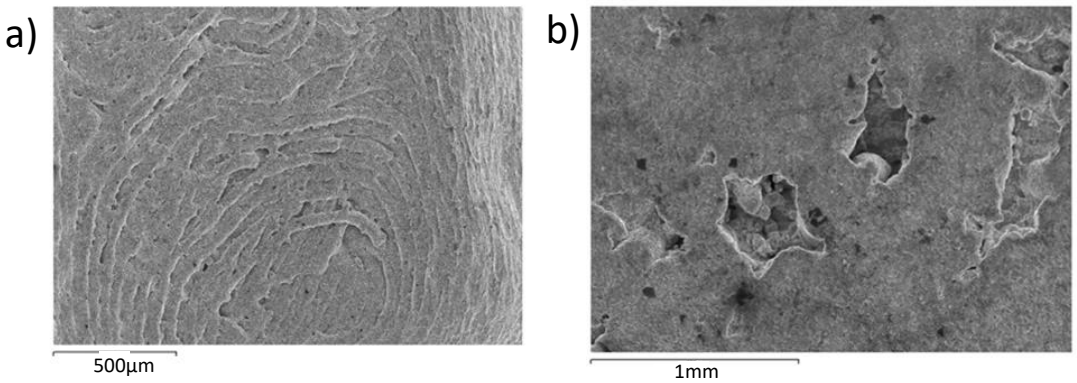

Figure 11. Surface defects of Laser sintered samples observed by SEM: a) welding seams produced along the sintering path, and b) Aligned microporosity with particles inside.

Microstructures of casted samples are shown in Figure 12a, in which typical dendritic morpholgy predominated. This color gardient in greyscale was due to the chemical composition

differences (chemical segregation) between diferent phases as a function of Cr and Co contents., The white second phase consisted on intermetallic precipitates very rich in W and Co, which were located along the interdendritic grain boundaries. Figure 12b shows SEM micrograph at high magnification, in which a surface pore with a crack inside has also been observed. The stress state in this defective area is high due to the residual stress accumulated by volume contraction (volumetric shrinkage) during the transformation from liquid to solid. This stress has been higher than the material strength and produced a crack.

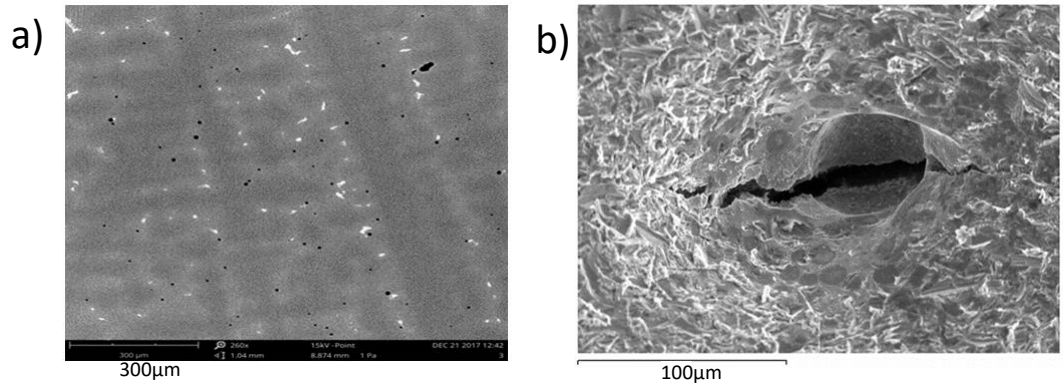

Figure 12. Microstructure and defects of Casted samples.

In the microstructure of the laser sintered samples, small precipitates which gave hardness to the material were observed. The size of these precipitates are fine and the quantities are lower than the casted samples. Figure 13 shows these white precipitates with their corresponding EDS-microanalysis which confirm precipitates formed by wolfram and Niobium. The black points are porosity.

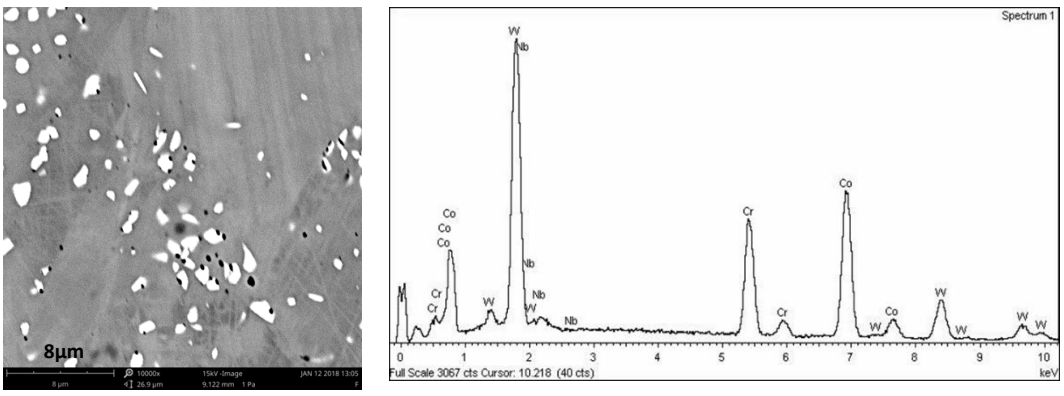

Figure 13. Microstructure of Laser sintered samples with white precipitates and EDS microanalysis of these precipitates.

A group of representative SEM images of the fractured surfaces after the 3-point bending test are shown in Figure 14. SEM fractographical analysis of CADCAM milled samples clearly showed a predominantly brittle fracture behavior, with facetted planes without plastic strain, as seen in (Fig. 14 a and b). Deep farrows have also been observed in fractured surfaces of CADCAM milled samples, as well as the presence of a large number of transverse and longitudinal secondary cracks randomly distributed.

Fractographic images of laser sintered samples showed mixed-fracture behavior, some areas with brittle fracture and others with plastic deformation, as seen in (Fig. 14 c and d). A non-linear type of crack propagation has been observed in laser sintered fractured surfaces. Consequently, fracture of laser sintered samples were sensible to microstructure, very similar to that seen with casted samples.

Fractographic observations of casted samples (Figure 14 e and f) presented a clear directionality of the fracture. The fractures were also sensitive to the microstructure. (if singular, the fracture was also sensitive to the microstructure) The crack propagation followed a dendritic orientation, as seen in (Fig. 13 e and f).

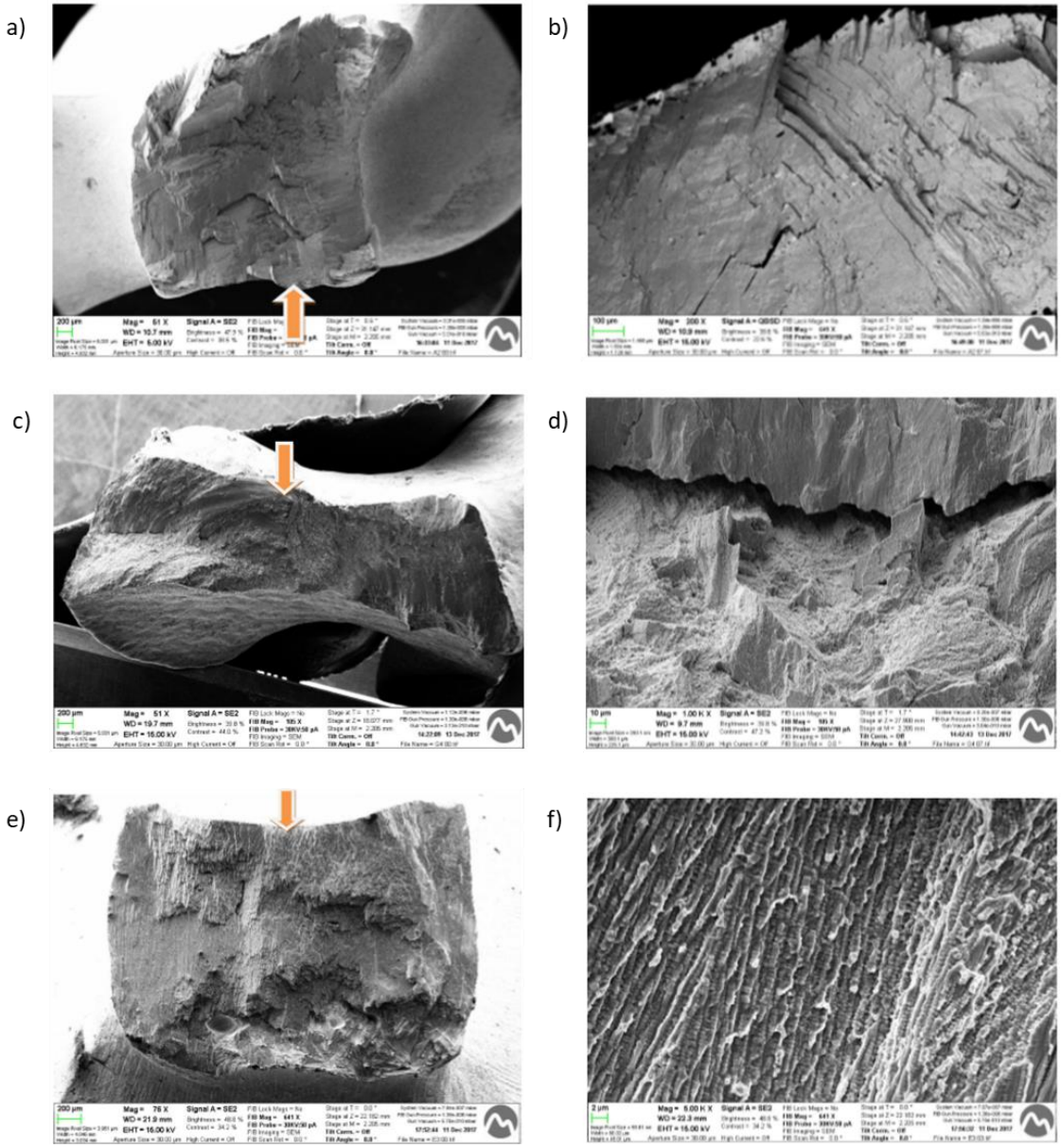

Figure 14. Fractographic images of mechanical tested samples. CADCAM milled samples with brittle fracture (a, b). Laser sintered samples with mixed fracture (c, d). Casted samples with detail of crack propagation with preferential directionality (e, f).

4. DISCUSSION

On the basis of the results obtained in marginal gap determination, CADCAM manufacturing method using programmable 5-axis automatic milling machine presented the highest level of accuracy in comparison to the other processes. This would be due to the ability of reproducing a 3D item from a 3D-CAD file. In contrast, traditional casting process by lost-wax method showed the lowest accuracy in terms of marginal fit. It is well known, the influence of both ability and experience of the laboratory technician to elaborate dental restorations have a crucial role in the quality of the end product. We should also take into consideration the defects caused by solidification (porous, volume contraction, chemical segregations….) are important disadvantages for the fidelity of the

prosthesis´ dimensions. Laser sintering process is somewhere in the middle, possessing advantages and limitations of both techniques. This manufacturing technique is also fully automated, but does not provide the accuracy levels achieved by CADCAM milling [56,64].

Cutting instruments (fine and sharp tools) are essential in achieving accuracy with the CADCAM Process. Nevertheless, this method also has some disadvantages such as material wastage, and wear, tear, and damage of the cutting tools during milling which increases lead to an increase in production costs. Laser sintering can produce samples with great accuracy of complex geometries where fine details are /(or) fine detail is necessary [65, 66]. However, porosity and chemical composition segregation resulting from the use of high melting temperatures are their main disadvantage. Regarding the final structures produced, inner porosity and geometric distortion levels produced by laser sintering were lower than casting technique. Sometimes the distortion unacceptable produced unacceptable discrepancies which were fixed through cutting and welding [66].

Base materials used as raw materials in CADCAM milling processes are free of pores and flaws developed due to casting [69-70]. The as-received materials have been cold-worked, treated with an annealing–heat treatment in order to eliminate the residual stresses, as well as increasing the density of the material through the removal of production defects. Consequently, CADCAM milled samples avoid the presence of defects associated with solidification mechanisms of Co–Cr alloys [67-69]. The absence of casting defects, together with the use of excellent cutting procedures, produce both, highest levels of accuracy and the best surface finishing as can be observed by Scanning Electron Microcopy and quantified by roughness values with statistical significance differences between each method used.

Microhardness results showed that laser sintered microstructures presented higher hardness values (473± 25) than casted samples (390 ± 15), whereas lowest value corresponded to CADCAM milled samples (356 ± 20). These results may be attributed to the finer distribution of the dispersed phase. It is well known that with both finer and dispersed phase, the material presents higher hardness due to increased obstacles for the mobility of dislocations. Casted samples showed the presence of this second dispersed phase in their microstructure (Figure 13) but the precipitates were bigger in size and presented in a lower quantity. This fact favors the dislocation mobility and hardness decrease. Besides, the microstructural grain size obtained by casting were higher than that produced by laser sintering due to the lower cooling process [68]. In addition, the presence of residual stresses during sintering is another possible explanation for the increased hardness [70-72]. CADCAM samples did not present a dispersed second phase in their microstructure with the exception of a few isolated clusters of precipitates. The material did not present residual stress due to the annealing treatment which relaxed stresses induced by milling

Takaichi et al. [66] showed that microstructure, porosity and mechanical properties are dependent not only on the alloy but also on the operational parameters. The addition of W and Mo in the chemical composition of Co-Cr alloys produces stabilization of crystalline phases with hexagonal close-packed structures (hcp). Also strengthen the alloy through the formation of Mo and W carbide; however recent studies have shown that the addition of W in Co-Cr alloys could suppress the formation of brittle and undesirable sigma (σ) phase, especially after the appropriate heat treatment.

In this study, the chemical composition was identical for each process. Therefore, it should be suggested that differences in the mechanical properties does not depend on elemental composition, but mainly depend on factors linked to the variations of the microstructure and defects related to manufacturing methods used. Laser sintering samples showed the highest values of hardness due to the dispersion of the fine precipitates, the presence of residual stresses and the small grain size. These properties are due to the manufacturing process.

However, the maximum flexure load to fracture corresponded to CAD-CAM milled samples, which could be explained by the absence of the extensive porosity. Porosity is undesirable, as it causes the mechanical properties to deteriorate and increases susceptibility to corrosion, such as crevice corrosion and pitting corrosion [28]. CADCAM milling provide structures with up to 100% nominal

density. However, laser sintered samples do not exceed 92-95%; these values are strongly dependent on the proper adjustment of operating conditions including laser power, temperatures, gas pressure, scan inter-spacing, as well as scan rate and thickness. The presence of a slight porosity and pore-free structures might explain the contradictory findings of the hardness in relation to the flexure load to fracture. Porosity is a well-known limitation of casted structures and is associated with the shrinkage of casting [73-74] and the gross dendritic structure of Co-Cr alloys during solidification producing the lowest results of flexural load to fracture.

The absence of porosity in manufactured structures produced by CADCAM milling method has a positive effect on their mechanical properties as well. Several researchers are currently investigating in order to implement knowledge and technology to increase the efficiency of laser sintering process. Indeed, some researchers are focusing their efforts to assess the effect of the laser beam orientation on the laser sintered components. The effect of the laser beam inclination on the laser sintered frameworks is still unknown to dentists and/or dental technicians. However, some studies indicate it is possible to produce structures with optimal orientations in order to provide maximum strengths in different directions due to the anisotropy [75-79].

5. CONCLUSIONS

Based on the findings of this study it can be considered that CADCAM milling process presents better marginal fit accuracy, surface quality (lower roughness) and higher flexure load to fracture as compared with laser sintering and casting methods. Casting and laser sintering showed porosity (inner and surface), residual stresses and chemical segregation in their microstructures, all of which play a key role in the mechanical properties. Casting and sintering conditions should be improved in order to enhance the microstructure and to avoid porosity to ensure optimal outcomes for clinical services.

ACKNOWLEDGEMENTS: In first place, the authors want to grateful to ARCHIMEDES company for the support in the research. This an example of the company which is involved in the research. The work was supported by the Spanish government and the Ministry of Science and Innovation of Spain by the research project number RTI2018-098075-B-C21 and RTI2018-098075-B-C22, cofounded by the EU through the European Regional Development Funds (MINECO-FEDER, EU). Authors also acknowledge Generalitat de Catalunya for the funding through 2017SGR-1165 project.

Conflicts of Interest: The authors declare no conflict of interest.

REFERENCES

1. Mormann, W.H.; Brandestini, M.; Lutz, F. The Cerec system: Computer-assisted preparation of direct ceramic inlays in 1 setting. Quintessenz 1987, 38, 457–470.
2. Sannino, G.; Germano, F.; Arcuri, L.; Bigelli, E.; Arcuri, C.; Barlattani, A. CEREC CAD-CAM Chairside System. Oral Implantol. 2015, 7, 57–70.
3. Mangano, F.; Gandolfi, A.; Luongo, G.; Logozzo, S. Intraoral scanners in dentistry: A review of the current literature. BMC Oral Health 2017, 17, 149.
4. Tapie L, Lebon N, Mawussi B, Fron Chabouis H, Duret F, Attal JP. Understanding dental CAD-CAM for restorations—the digital workflow from a mechanical engineering viewpoint. Int J Comput Dent. 2015; 18:21–44.
5. Tinschert J, Natt G, Hassenpflug S, Spiekermann H. Status of current CAD-CAM technology in dental medicine. Int J Comput Dent. 2004; 7:25–45.
6. Zimmermann M, Mehl A, Mörmann WH, Reich S. Intraoral scanning systems - a current overview. Int J Comput Dent. 2015;18(2):101-29.
7. Rekow ED. Dental CAD-CAM systems. What is the state of the art?. J Am Dent Assoc. 1991; 122(12):42-8.
8. Rekow ED, Erdman AG, Riley DR, Klamecki B. CAD-CAM for dental restorations--some of the curious challenges. IEEE Trans Biomed Eng. 1991; 38(4):314-8.
9. Rödiger, M.; Schneider, L.; Rinke, S. Influence of Material Selection on the Marginal Accuracy of CAD-CAM-Fabricated Metal- and All-Ceramic Single Crown Copings. Biomed. Res. Int. 2018, 2018, 2143906.

10. Sannino, G.; Gloria, F.; Schiavetti, R.; Ottria, L.; Barlattani, A. Dental wings CAD-CAM system precision: An internal and marginal fit sperimental analisys. Oral and Implantology. Oral Implantol. 2009, 2, 11–20. 28.
11. Mah, J. K., Huang, J. C., & Choo, H. Practical Applications of Cone-Beam Computed Tomography in Orthodontics. The Journal of the American Dental Association, 2010; 141, 7S–13S. doi: 10.14219/jada.archive.2010.0361
12. Hong, J.-S., Oh, K.-M., Kim, B.-R., Kim, Y.-J., & Park, Y.-H. Three-dimensional analysis of pharyngeal airway volume in adults with anterior position of the mandible. American Journal of Orthodontics and Dentofacial Orthopedics, 2011; 140(4), e161–e169. doi:10.1016/j.ajodo.2011.04.020
13. Macleod, I., Heath, N. Cone-Beam Computed Tomography (CBCT) in Dental Practice. Dental Update, 2008; 35(9), 590–598. doi:10.12968/ denu.2008.35.9.590.
14. Scarfe, W. C., Levin, M. D., Gane, D., & Farman, A. G. Use of Cone Beam Computed Tomography in Endodontics. International Journal of Dentistry, 2009, 1–20. doi:10.1155/2009/634567.
15. Quereshy, F. A., Savell, T. A., & Palomo, J. M. Applications of Cone Beam Computed Tomography in the Practice of Oral and Maxillofacial Surgery. Journal of Oral and Maxillofacial Surgery, 2008; 66(4), 791–796. doi: 10.1016/j.joms.2007.11.018
16. Swain, M. V., Xue, J. State of the Art of Micro-CT Applications in Dental Research. International Journal of Oral Science, 2009; 1(4), 177–188. doi:10.4248/ijos09031
17. Dong, G., Dong, Q., Liu, Y., Lou, B., Feng, J., Wang, K.,Wu, H. High-resolution micro-CT scanning as an innovative tool for evaluating dental hard tissue development. Journal of Applied Clinical Medical Physics, 2014; 15(4), 335–344. doi:10.1120/ jacmp. v15i4.4956
18. Ortorp A, Jörnsson D, Mouhsen A, Vult von Steyern P. The fit of cobalt- chromium three-unit fixed dental prostheses fabricated with four different techniques: a comparative in vitro study. Dent Mater 2011; 27:356-63.
19. Cho, S.H.; Schaefer, O.; Thompson, G.A.; Guentsch, A. Comparison of accuracy and reproducibility of casts made by digital and conventional methods. J. Prosthet. Dent. 2015, 113, 310–315.
20. Eh, N.A.N.; Mack, F.; Evans, J.; Mackay, J.; Hatamleh, M.M. Accuracy and reliability of methods to measure marginal adaptation of crowns and FDPs: A literature review. J. Prosthodont. 2013, 22, 419–428. 12.
21. Koutsoukis T, Zinelis S, Eliades G, Al-Wazzan K, Rifaiy MA, Al Jabbari YS. Selective laser melting technique of Co-Cr dental alloys: a review of structure and properties and comparative analysis with other available techniques. J Prosthodont 2015; 24:303-12.
22. Sofia D, Barletta D, Poletto M. Laser sintering process of ceramic powders. Additive Manufacturing 2018, 23: 215-224.
23. Sofia D, Granese M Barletta D, Poletto M. Laser sintering of unimodal distributed glass powders of different size. Proced. Eng. 2015, 102: 749-758.
24. Ferreira TJ, Vieira MT, Costa J, Gato PT. Manufacturing Dental Implants using Powder Injection Molding. J Orthod Endod. 2016, 2:1.
25. Ataee A, Li Y, Song G, Wen C. Metal scaffolds processed by electron beam melting for biomedical applications. In Metallic Foam Bone. Processing, Modification and Characterization and Properties. Elsevier. London. 2017: 83-110.
26. Suresh G, Narayana L, Kedar M. Laser Engineered Net Shaping Process in Development of Medical Implants: An Overview. J. Adv.Res.Dynam.Control Syst. 2017, 9(14):745-756
27. Hero H, Syverud M, Gjonnes J, Horst JA. Ductility and structure of some cobalt-base dental casting alloys.Biomaterials 1984;5:201–8.
28. Qiu J, Yu WQ, Zhang FQ, Smales RJ, Zhang YL, Lu CH.Corrosion behaviour and surface analysis of a Co–Cr andtwo Ni–Cr dental alloys before and after simulated porcelainfiring. Eur J Oral Sci 2011; 119:93–101
29. Lewis AJ: Radiographic evaluation of porosities in removable partial denture castings. J Prosthet Dent 1978; 39:278-281
30. van Noort R, Lamb DJ: A scanning electron microscope study of Co-Cr partial dentures fractured in service. J Dent 1984; 12:122-126.
31. Naert, I.; van Der Donck, A.; Beckers, L. Precision of fit and clinical evaluation of all-ceramic full restorations followed between 0.5 and 5 years. J. Oral Rehabil. 2005, 32, 51–57.
32. Sorensen SE, Larsen IB, Jorgensen KD: Gingival and alveolar bone reaction to marginal fit of subgingival crown margins. Scand J Dent Res 1986; 94:109-114.

33. Felton DA, Kanoy BE, Bayne SC, et al: Effect of in vivo crown margin discrepancies on periodontal health. J Prosthet Dent 1991; 65:357-364.
34. Jacobs MS, Windeler AS: An investigation of dental luting cement solubility as a function of the marginal gap. J Prosthet Dent 1991; 65:436-442.
35. Martins LM, Lorenzoni FC, Melo AO, Silva LM, Oliveira JL, Oliveira PC. Internal fit of two all-ceramic systems and metal-ceramic crowns. J Appl Oral Sci 2012; 20:235-40.
36. Kim BC, Kim WC, Kim HY, Kim JH. Evaluation of the marginal and internal gap of metal-ceramic crown fabricated with a selective laser sintering technology: two- and three-dimensional replica techniques. J Adv Prostho- dont 2013; 5:179-86.
37. Christensen GJ: Marginal fit of gold inlay castings. J Prosthet Dent 1966; 16:297-305.
38. Baldissara P, Baldissara S, Scotti R: Reliability of tactile perception using sharp and dull explorers in marginal opening identification. Int J Prosthodont 1998; 2:591-594.
39. Jahangiri L, Wahlers C, Hittelman E, et al: Assessment of sensitivity and specificity of clinical evaluation of cast restoration marginal accuracy compared to stereomicroscopy. J Prosthet Dent 2005; 93:138-142.
40. Tan PL, Gratton DG, Diaz-Arnold AM, Holmes DC. An in vitro comparison of vertical marginal gaps of CAD-CAM titanium and conventional cast restorations. J Prosthodont. 2008; 17(5):378-83.
41. Leong D, Chai J, Lautenschlager E, Gilbert J. Marginal fit of machine-milled titanium and cast titanium single crowns. Int J Prosthodont. 1994; 7(5):440-7
42. Martinez-Rus, F.; Ferreiroa, A.; Ozcan, M.; Pradies, G. Marginal discrepancy of monolithic and veneered all-ceramic crowns on titanium and zirconia implant abutments before and after adhesive cementation: A scanning electron microscopy analysis. Int. J. Oral Maxillofac. Implants 2013, 28, 480–487.
43. Nedelcu, R.; Olsson, P.; Nyström, I.; Thor, A. Finish line distinctness and accuracy in 7 intraoral scanners versus conventional impression: An in vitro descriptive comparison. BMC Oral Health 2018, 18, 27.
44. Aldegheishem, A.; Ioannidis, G.; Att, W.; Petridis, H. Success and survival of various types of all-ceramic single crowns: A critical review and analysis of studies with a mean follow-up of 5 years or longer. Int. J. Prosthodont. 2017, 30, 168–181.
45. Rinke, S.; Fornefett, D.; Gersdor, N.; Lange, K.; Roediger, M. Multifactorial analysis of the impact of different manufacturing processes on the marginal t of zirconia copings. Dent. Mater. 2012, 31, 601–609.
46. McLean, J.W.; von Fraunhofer, J.A. E Estimation of cement lm thickness by an in vivo technique. Br. Dent. J. 1971, 131, 107–111.
47. Contrepois, M.; Soenen, A.; Bartala, M.; Laviole, O. Marginal adaptation of ceramic crowns: A systematic review. J. Prosthet. Dent. 2013, 110, 447–454.
48. Song TJ, Known TK, Yang JH, Han SH, Lee JB, Kim SH, Yeo IS. Marginal fit of anterior 3-unit fixed partial zirconia restorations using different CAD-CAM systems. J. Adv. Prosthodont 2013, 5:219-225.
49. Lövgren N, Roxner R, Klemendz S, Larsson C. Effect of production method on surface roughness, marginal and internal fit, and retention of cobalt-chromium single crowns. J Prosth Dent. 2017;118(1):95-101.
50. Hama Suleiman S, Vult von Steyern P: Fracture strength of porcelain fused to metal crowns made of cast, milled or laser-sintered cobalt-chromium. Acta Odontol Scand 2013; 71:1280-1289.
51. Reclaru L, Ardelean L, Rusu L, et al: Co-Cr material selection in prosthetic restoration: Laser sintering Technology. Solid State Phenomena 2012; 188:412-415.
52. Boitelle P, Mawussi B, Tapie L, Fromentin O. A systematic review of CAD-CAM fit restoration evaluations. J Oral Rehabil 2014; 41:853–74.
53. Wiskott HW, Belser UC, Scherrer SS. The effect of film thickness and surface texture on the resistance of cemented extra coronal restorations to lateral fatigue loading. Int J Prosthodont 1999; 12:255-62.
54. Juntavee N, Millstein PL. Effect of surface roughness and cement space on crown retention. J Prosthet Dent 1992; 68:482-6.
55. Tinschert J, Natt G, Hassenpflug S, Spiekermann H. Status of current CAD-CAM technology in dental medicine. Int J Comput Dent 2004; 7:25–45.
56. Castillo-Oyague R, Osorio R, Osorio E, et al: The effect of surface treatments on the microroughness of laser-sintered and vacuum-cast base metal alloys for dental prosthetic frameworks. Microsc Res Tech 2012; 75:1206-1212.
57. Han X, Sawada T, Schille C, Schweizer E, Scheidler L, Geis-Gerstofer J, Rupp F, Spintzyk F. Comparative Analysis of Mechanical Properties and Metal-Ceramic Bond Strength of Co-Cr Dental Alloy Fabricated by Different Manufacturing Processes. Materials 2018. Doi. 103390/ma11101801

58. Holmes JR, Bayne SC, Holland GA, Sulik WD, Considerations in measurement of marginal fit. J.Prosthet. Dent. 1989; 62:405-407
59. Affy A, Haney S, Verrett R, Mansueto M, Cray J, Johnson R, Marginal discrepancy of noble-ceramic fixed dental prosthesis frameworks fabricated by conventional and digital technologies. J Prosthet. Dent 2018; 119:307.
60. Kim HR, Jang SH, Kim YK, Son JS, Min BK, Kim KH, Kwon TY. Microstructures and Mechanical Properties of Co-Cr Dental Alloys Fabricated by Three CAD/CAM-Based Processing Techniques. Materials 2016, 9, 596; doi:10.3390/ma9070596.
61. Chan, C.-W., Smith, G., & Lee, S. (2018). A Preliminary Study to Enhance the Tribological Performance of CoCrMo Alloy by Fibre Laser Remelting for Articular Joint Implant Applications. Lubricants, 6(1), 24. doi:10.3390/lubricants6010024
62. Balla, V. K., Bodhak, S., Bose, S., & Bandyopadhyay, A. (2010). Porous tantalum structures for bone implants: Fabrication, mechanical and in vitro biological properties. Acta Biomaterialia, 6(8), 3349–3359. doi:10.1016/j. actbio.2010.01.046.
63. Dikova T. Bending fracture of Co-Cr dental bridges, produced by additive technologies: experimental investigation. Procedia Structural Integrity 13 (2018) 461–468. https://doi.org/10.1016/j.prostr.2018.12.077
64. Hong MH, Min BK, Kwon TY. Fabricating High-Quality 3D-Printed Alloys for Dental Applications. Appl. Sci. 2017, 7, 710; doi:10.3390/app7070710.
65. Sing, S. L., An, J., Yeong, W. Y., & Wiria, F. E. (2015). Laser and electron-beam powder-bed additive manufacturing of metallic implants: A review on processes, materials and designs. Journal of Orthopaedic Research, 34(3), 369–385. doi:10.1002/jor.23075
66. Takaichi A, Suyalatu, Nakamoto T, et al: Microstructures and mechanical properties of Co-29Cr-6Mo alloy fabricated by selective laser melting process for dental applications. J Mech Behav Biomed Mater 2013; 21:67-76
67. Munoz AI, Mischler S: Effect of the environment on wear ranking and corrosion of biomedical CoCrMo alloys. J Mater Sci Mater Med 2011; 22:437-450
68. Dharmar S, Rathnasamy RJ, Swaminathan TN: Radiographic and metallographic evaluation of porosity defects and grain structure of cast chromium cobalt removable partial dentures. J Prosthet Dent 1993; 69:369-373.
69. Rodrigues WC, Broilo LR, Schaeffer L, et al: Powder metallurgical processing of Co-28%Cr-6%Mo for dental implants: physical, mechanical and electrochemical properties. Powder Technol 2011; 206:233-238.
70. Shiomi M, Osakada K, Nakamura K, et al: Residual stress within metallic model made by selective laser melting process. Cirp Ann-Manuf Techn 2004; 53:195-198
71. Reclaru L, Susz C, Ardelean L: Laser beam welding. Timisoara Med J 2010;60:86-89
72. Jang SH, Lee DH, HA JY, Hanawa T, Kim, KH, Kwon T. Preliminary evaluation of mechanical properties of Co-Cr alloys fabricated by three manufacturing processes. Int J Prosthodont 2015; 28: 396-398.
73. Al Jabbari YS, Koutsoukis T, Barmpagadaki X, et al.: Metallurgical and interfacial characterization of PFM Co-Cr dental alloys fabricated via casting, milling or selective laser melting. Dent Mater 2014; 30:e79-88
74. Simchi A, Pohl H: Effects of laser sintering processing parameters on the microstructure and densification of iron powder. Mat Sci Eng a-Struct 2003; 359:119-128.
75. Sailer, I.; Makarov, N.A.; Thoma, D.S.; Zwahlen, M.; Pjetursson, B.E. All-ceramic or metal-ceramic tooth-supported fixed dental prostheses (FDPs)? A systematic review of the survival and complication rates. Part I: Single crowns (SCs). Dent. Mater. 2015, 31, 603–623.
76. Wolfart, S.; Wegner, S.F.; Al-Halabi, A.; Kern, M. Clinical evaluation of marginal fit of a new experimental all-ceramic system before and after cementation. Int. J. Prosthodont. 2003, 16, 587e92.
77. Oyague RC, Sanchez-Turrion A, Lopez-Lozano JF, et al: Vertical discrepancy and microleakage of laser-sintered and vacuum-cast implant-supported structures luted with different cement types. J Dent 2012; 40:123-130
78. Kruth JP, Vandenbroucke B, Van Vaerenbergh J. Benchmarking of different SLS/SLM processes as rapid manufacturing techniques. Int Conf Polymers Moulds Innovations (PMI). Gent, Belgium, 2005. In: Proceedings of the PMI, paper 525. http://doc.utwente.nl/52902/ Access date 20 May 2013
79. Ucar Y, Akova T, Akyil MS, et al: Internal fit evaluation of crowns prepared using a new dental crown fabrication technique: laser-sintered Co-Cr crowns. J Prosthet Dent 2009; 102:253-259

614